Estimating Damping in Microresonators by Measuring Thermomechanical Noise Using Laser Doppler Vibrometry

Ottoleo Kuter-Arnebeck, Aleksander Labuda, Surabhi Joshi, Kaushik Das, and Srikar Vengallatore

***Abstract*— The fluctuation-dissipation theorem establishes the fundamental links between thermomechanical noise and damping. In this paper, we bridge the gap between theory and practice by developing protocols for estimating dissipation in low-loss microresonators by measuring thermomechanical noise using laser Doppler vibrometry. The measurement does not require external actuation of the device and damping can be estimated without relying upon knowledge of material properties, device dimensions, or structural stiffness. The power spectral density of velocity and displacement noise is computed using a direct method that avoids segmenting the measurements in the time domain, thereby avoiding any bias in the estimation of the quality factor. We demonstrate the implementation of the protocol by measuring damping at room temperature and low pressure in four silicon-based microcantilever resonators with natural frequencies ranging from 17.6 to 26.7 kHz and quality factors ranging from 2×10^4 to 2×10^5. The accuracy of noise-based estimates is evaluated by comparison with values of the log decrement measured under free decay. [2013–0127]**

***Index Terms*— MEMS, microresonators, damping, thermomechanical noise, laser Doppler vibrometry.**

I. Introduction

MEASURING and controlling damping is essential for the design and development of resonant microsystems (MEMS) that are used for sensing, vibration energy harvesting, signal processing, precision measurements, and materials characterization (see, for example [1], [2]). A direct measurement of dissipation or entropy generation is difficult; instead, damping is measured by monitoring the dynamics of the oscillating structure. Three methods are commonly used: (i) subject the system to time harmonic excitation and measure the phase angle, ϕ, by which the excitation leads the response; (ii) subject the system to time harmonic excitation and measure the quality factor, Q, from the half-power bandwidth of resonance at steady-state; and (iii) permit the structure to oscillate freely after an initial impulsive excitation and measure the log decrement, δ, from the decaying amplitude [3]. These measures can be related to each other, and to energy dissipation, when damping is *small* ($\phi < 0.1$) and *linear* (that is, the magnitude of dissipation is independent of the amplitude of oscillation). To an excellent approximation [3], [4],

$$\phi = Q^{-1} = \frac{\delta}{\pi} = \frac{\Delta W}{2\pi W}, \tag{1}$$

where ΔW is the energy dissipated per cycle and W is the maximum elastic energy in the structure during the vibration cycle. For all three methods, the measurement requires the structure to be actuated, either by integrating an actuator with the microsystem or by employing a shaker. This requirement can pose practical difficulties, especially for devices with complicated geometries and mode shapes, and introduce undesirable nonlinearities in the response of the microsystem.

In this paper, we study a technique that does not require any external actuation. The essential idea is to estimate damping by measuring thermomechanical noise (also called *mechanical-thermal noise*). The link between thermomechanical noise and damping is established by the Fluctuation-Dissipation Theorem [5], [6]. A qualitative and intuitive understanding may be gained by viewing dissipation as a means of energy transfer from the mechanical structure to its thermal environment (or thermal reservoir), and from the reservoir to the structure. When a periodic force is applied on the structure, mechanical energy is converted to heat due to damping during each cycle of vibration. The structure can maintain its equilibrium temperature by transferring heat to the many microscopic degrees-of-freedom of the reservoir. Conversely, in the absence of any external force, the structure will exhibit spontaneous random displacements around its equilibrium position due to an injection of energy from the reservoir.

The Fluctuation-Dissipation Theorem can be combined with the Equipartition Theorem to express thermomechanical noise as a function of damping [5]–[8]. Such expressions have been used to estimate the effects of damping on device performance (see, for example, [2], [9]), but the inverse problem of estimating damping by measuring thermomechanical noise has received relatively little attention, particularly for characterizing low-loss high-Q micromechanical resonators that are of interest for many applications. Any measurement of noise invariably contains contributions from several sources (building vibrations, electrical line noise, electronic noise, optical noise), and every contribution must be identified and

Manuscript received April 24, 2013; revised August 19, 2013; accepted October 7, 2013. Date of publication October 30, 2013; date of current version May 29, 2014. This work was supported in part by the Natural Sciences and Engineering Research Council of Canada and in part by the Canada Research Chairs program. Subject Editor D. DeVoe.

O. Kuter-Arnebeck, S. Joshi, and S. Vengallatore are with the Department of Mechanical Engineering, McGill University, Montreal, QC H3A 2K6, Canada (e-mail: ottoleo.kuter-arnebeck@mail.mcgill.ca; surabhi.joshi@mail.mcgill.ca; srikar.vengallatore@mcgill.ca).

A. Labuda is with Asylum Research, Santa Barbara, CA 93117 USA (e-mail: aleks.labuda@gmail.com).

K. Das is with the MiQro Innovation Collaborative Centre, Bromont, QC J2L 1S8, Canada (e-mail: kaushik.das@mail.mcgill.ca).

Color versions of one or more of the figures in this paper are available online at http://ieeexplore.ieee.org.

Digital Object Identifier 10.1109/JMEMS.2013.2286199

taken into account in order to determine the thermomechanical noise spectrum. Some sources can be eliminated by design (for example, using air tables to isolate the specimen from building vibrations) and others (such as electronic and optical noise) can be excluded by signal processing.

Thermomechanical noise can be measured using custom-built laser interferometers [10]–[13], position sensitive photodetectors (in the configuration commonly employed in atomic force microscopes) [14]–[19], and laser Doppler vibrometers [20]–[24]. Laser Doppler vibrometry (LDV) is a high-precision, non-contact interferometric technique and commercial vibrometers are available for characterizing the out-of-plane modes of micromechanical structures [25]. LDV is now widely used to study the dynamics of MEMS; for example, the stiffness of micromachined cantilevers used for scanning probe microscopy can be estimated by measuring thermomechanical noise using LDV [21]–[24]. It is therefore timely to extend these capabilities to noise-based estimation of damping in high-Q microresonators.

The remaining sections of this paper are organized as follows. Section II establishes the theoretical foundations of the technique and presents a protocol for estimating damping from thermomechanical noise. The protocol is implemented by measuring damping in a set of four silicon-based microcantilever resonators with natural frequencies ranging from 17.6 to 26.7 kHz. The accuracy of noise-based estimates is assessed by comparison with values of the log decrement obtained under free decay. Section III describes the microfabrication and characterization of the devices; Section IV explains the methods used for measurement and analysis of noise; and Section V presents the main results of our study.

II. Theoretical Foundations

Let us consider the vibrations of a single mode of a linear microresonator. The elastic response can be modeled using a point mass m and a massless linear spring with stiffness k. The displacement of the mass at time t is designated $x(t)$, and we seek the value of damping at the natural frequency $f_0 = (1/2\pi)\sqrt{k/m}$. We assume that damping is small ($\phi < 0.1$) and linear. Dissipation can be introduced into the model by adding a viscous dashpot with a damping coefficient c that is independent of frequency so that $Q = \sqrt{mk}/c = 2\pi\, m\, f_0/c$ [3]. Alternately, the dynamics of the mode can be modeled using a point mass and a complex spring with stiffness $k^* = k[1 + i\,\phi(f)]$. Two cases are of particular interest for MEMS: (i) the *Kimball–Lovell solid* [4] with ϕ independent of frequency, f, which is a good approximation over many decades of frequency for internal friction due to defect-induced anelasticity [26], [27]; and (ii) the *Zener solid* (also called the *standard anelastic solid*) with a single relaxation peak of the form [3]

$$\phi(f) = \Delta \frac{2\pi f \tau}{1 + (2\pi f \tau)^2}, \tag{2}$$

where Δ and τ are the characteristic relaxation strength and relaxation time, respectively. Examples of mechanisms that exhibit a single relaxation peak include thermoelastic damping in monolithic beams [28], [29], Akhiezer damping [30], and Gorsky damping [31]. The phase angle and quality factor are related to each other, and to the log decrement, by Eq. (1).

Now, let the resonator establish thermodynamic equilibrium by interacting with a heat reservoir. According to the Fluctuation-Dissipation Theorem, the presence of dissipation in the mechanical system will lead to spontaneous random fluctuations of the value of $x(t)$ [5], [6]. The displacement noise can be conveniently analyzed in the frequency domain using the power spectrum. Denoting the Fourier transform of $x(t)$ by $X(f)$, the one-sided power spectral density (PSD) is $S_x(f) = 2|X(f)|^2$ with units of m^2/Hz. Following the approach of Saulson [7] and Levin [8], the PSD of displacement noise can be expressed as

$$S_x(f) = \frac{k_\mathrm{B} T}{\pi^2 f^2} \left|\Re[Y(f)]\right|, \tag{3}$$

where k_B is Boltzmann's constant, T is the absolute temperature, $\Re$ denotes the real part of a complex function, and $Y(f)$ is the mechanical admittance obtained by computing the response $x_1(t)$ when a force $F_1(t)$ is applied to the mass. If $X_1(f)$ and $F_1(f)$ denote the Fourier transforms of the displacement and force, respectively, then

$$Y(f) = i\, 2\pi f\, \frac{X_1(f)}{F_1(f)}. \tag{4}$$

The mechanical admittance can be readily computed by applying a time-harmonic force on the mass. Accordingly, for viscous damping,

$$S_x(f) = \frac{2k_\mathrm{B} T}{\pi k\, f_0} \frac{\left(\frac{1}{Q}\right)}{\left(1-\Omega^2\right)^2 + \left(\frac{\Omega}{Q}\right)^2}; \tag{5}$$

and for the complex spring,

$$S_x(f) = \frac{2k_\mathrm{B} T}{\pi k\, f_0} \frac{\left(\frac{\phi(f)}{\Omega}\right)}{\left(1-\Omega^2\right)^2 + [\phi(f)]^2}. \tag{6}$$

In these expressions, $\Omega = (f/f_0)$ is the non-dimensional frequency ratio.

Equations (5) and (6) provide a direct and explicit link between thermomechanical noise and damping. Further, in the vicinity of the natural frequency ($\Omega \simeq 1$), both expressions reduce to a simple Lorentzian function given by

$$S_x(f) \simeq \frac{k_\mathrm{B} T}{\pi\, k} \frac{\left(\frac{f_0}{2Q}\right)}{(f-f_0)^2 + \left(\frac{f_0}{2Q}\right)^2} \simeq \frac{k_\mathrm{B} T}{\pi\, k} \frac{\left(\frac{f_0\,\phi}{2}\right)}{(f-f_0)^2 + \left(\frac{f_0\,\phi}{2}\right)^2} \tag{7}$$

Expressions for the PSD of velocity noise can be obtained from (5)–(7) by noting that

$$S_\mathrm{v}(f) = 4\pi^2 f^2 S_x(f) \tag{8}$$

As an illustrative example, consider the effects of damping on thermomechanical noise for a microresonator with a stiffness of 10 N/m and natural frequency of 20 kHz (Figure 1). The PSD was computed by setting $Q = \phi^{-1} = 3 \times 10^4$ in Equations (5) and (6) for viscous damping and the Kimball–Lovell solid, respectively. For the standard anelastic solid,

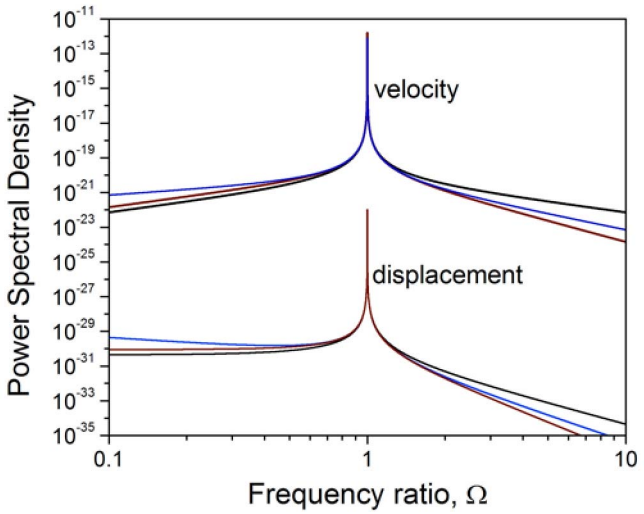

Fig. 1. Power spectral density of displacement (in units of m^2/Hz) and velocity (in units of $(m/s)^2$/Hz) for a representative microresonator with stiffness of 10 N/m, natural frequency of 20 kHz, and quality factor of 3×10^4. Three different models for damping are shown: viscous damping is denoted by the black curves; Kimball–Lovell solid (complex spring with ϕ independent of frequency) by the blue curves; and the standard anelastic solid by the red curves.

the values of Δ and τ were chosen to obtain $\phi^{-1} = 3 \times 10^4$ at 20 kHz. As expected, the curves collapse to a single peak at resonance ($\Omega = 1$).

Equations (7) and (8) suggest a simple protocol for estimating damping at the natural frequency: (i) measure the time series of noise associated with displacement or velocity; (ii) compute the power spectral density; and (iii) fit the resonance peak to obtain $Q = \phi^{-1}$. Values of beam geometry, material property or structural stiffness are not required for measurement or analysis, and damping can be estimated without detailed knowledge of the underlying mechanisms of dissipation.

III. Materials and Structures

Four high-Q microcantilever devices with fundamental natural frequencies ranging from 17.6 to 26.7 kHz were selected for measurement and analysis. The cantilevers are attached monolithically to a large supporting frame. Specimen 1 is a bare silicon microcantilever. Specimens 2 to 4 are composite structures consisting of an array of aluminum nanowires patterned on one surface of silicon microcantilevers. The array is patterned at the root of the microcantilever with the nanowires oriented along the axis of the silicon beam. The length of each nanowire is 20% that of the silicon beam. The thickness of the nanowires ranges from 50 to 100 nm, the width from 100 to 400 nm, and the center-to-center spacing between adjacent nanowires is 1 μm. The microfabrication and characterization of the microresonators have been described in detail previously [27], [32]–[36], and the salient points are summarized below.

A. Microfabrication and Nanopatterning

The microcantilevers were micromachined using deep reactive-ion etching (DRIE) of double-side polished, (100)-oriented commercial grade silicon-on-insulator (SOI) wafers. The device layer defined the thickness of the microcantilevers, the buried-oxide layer served as an etch stop, and the handle layer formed the supporting frame. The first step was to grow 500 nm thick layers of silicon dioxide on both surfaces of the SOI wafers using wet oxidation at 1100 °C. A standard photolithography and etching process was implemented to pattern the oxide film on top of the device layer. A 10 μm thick layer of a positive photoresist (AZ9245, AZ Electronic Materials) was spin-coated on this surface and patterned. Using the silicon dioxide and photoresist bilayer as a hard mask, the device layer was etched by DRIE and then cleaned using oxygen plasma. Subsequently, 100 nm thick silicon oxide layers were grown on all exposed silicon surfaces by placing the wafer in a furnace. The handle layer was then patterned and etched using a combination of dry etching with DRIE and wet etching using tetramethyl ammonium hydroxide (TMAH) to release the microcantilevers. Finally, the structures were dipped in HF to remove the silicon oxide from all surfaces of the silicon microcantilevers.

Specimen 1 did not require any further processing. Specimens 2 to 4 were metalized by patterning an array of aluminum nanowires using a lift-off process implemented using electron-beam lithography. The microcantilevers were spray-coated with a 390 nm thick layer of a copolymer (MMA-MAA EL11 (Microchem, Inc.) that was diluted with methyl isobutyl ketone, and then baked at 150 °C for 90 seconds. Subsequently, the structures were spray coated with 200 nm of electron beam resist (PMMA A2, Microchem, Inc.) and baked at 180 °C for 90 seconds. The bilayer-resist-coated microcantilevers were patterned using electron beam lithography (Hitachi FEGSEM SU-70) operating at 30 kV with beam current of 357 pA and electron doses in the range of 6–8 nC/cm. After development, the lift-off process was implemented by depositing thin films of aluminum using electron-beam evaporation at a rate of 0.2 nm/s. The nanowires exhibit a columnar grain structure; the in-plane grain diameter is lognormally distributed with a median value that is approximately equal to the thickness of the nanowire [33].

B. Measurement of Log Decrement

The log decrement was measured at room temperature (23 °C) and low pressure (4×10^{-3} Pa) using laser Doppler vibrometry. The supporting frame was mounted on a precision-machined stainless steel clamp, attached to a shaker (NanoOP65, Mad City Labs Inc, WI, USA), and placed inside a vacuum chamber. The sensor unit consists of a laser head equipped with a 633 nm helium-neon laser and a built-in camera (OFV534 fiber coupled vibrometer sensor head, Polytec, Germany), and a digital velocity decoder (OFV5000 VD09 decoder) to process the voltage output from the sensor. The output of the LDV was captured using a data acquisition card (NI USB-6211, National Instruments Corp., USA) and recorded in LabVIEW (National Instruments Corp., USA). The laser beam has a diameter of 40 μm at a standoff distance of 30 cm, allowing the LDV to be positioned outside the vacuum chamber. A pneumatic vibration isolation table (RP Reliance,

TABLE I
GEOMETRY, NATURAL FREQUENCY, AND DAMPING OF THE MICROCANTILEVER DEVICES. SPECIMEN 1 IS A BARE SILICON MICROCANTILEVER. SPECIMENS 2 TO 4 ARE COMPOSITE STRUCTURES CONSISTING OF AN ARRAY OF ALUMINUM NANOWIRES PATTERNED AT THE ROOT OF SILICON MICROCANTILEVERS. THE DIMENSIONS OF THE NANOWIRES ARE NOT SHOWN IN THE TABLE

	Dimensions of silicon microcantilevers			Natural frequency	Log decrement, δ ($\pm 7\%$)	$Q = \pi \delta^{-1}$ ($\pm 7\%$)
	Length	Width	Thickness			
Specimen 1	630 μm	300 μm	8.0 μm	26,749 Hz	1.63×10^{-5}	19.3×10^{4}
Specimen 2	750 μm	300 μm	8.5 μm	21,046 Hz	5.8×10^{-5}	5.40×10^{4}
Specimen 3	765 μm	300 μm	8.0 μm	19,160 Hz	2.7×10^{-5}	11.6×10^{4}
Specimen 4	750 μm	300 μm	7.5 μm	17,664 Hz	1.3×10^{-4}	2.40×10^{4}

Newport Corp, USA) was used to isolate the chamber and measurement apparatus from ambient ground vibrations and pumping systems.

The microcantilever was excited at a frequency close to, but less than, the fundamental natural frequency using the shaker. The amplitude of vibration was controlled to ensure that the strain in the structure was less than 10^{-5}. The excitation was terminated and the free decay of the beam was recorded and analyzed to obtain the log decrement. The results of the measurements are presented in Table I. The last column shows the effective quality factor calculated using Eq.(1). Multiple studies of the precision of our apparatus ($\sim$100 measurements, each consisting of a complete remount and pump down) indicate that the maximum fractional uncertainty in damping is 7% [27], [32]–[36]. Damping in the bare silicon microcantilever (Specimen 1) is due to thermoelastic damping and clamping losses [32], [35]. For Specimens 2, 3 and 4, metallization due to aluminum leads to much higher dissipation due to grain-boundary sliding; hence, damping is a function of the thickness, width, and grain size distribution of the aluminum nanowires [27].

IV. MEASUREMENT AND ANALYSIS OF NOISE

A. Measurement of Velocity Time Series

Thermomechanical noise was measured at room temperature (23 °C) and low pressure (4×10^{-3} Pa) using the apparatus and instruments described in the previous section, but without employing the shaker. Instead, the device was mounted on the precision-machined clamps and installed inside the vacuum chamber. The velocity of the tip of the microcantilever was monitored using the LDV without applying any external actuation. Each measurement consisted of recording the velocity time series for 90 seconds at a sampling frequency, f_s, of 100 kHz. These values were chosen to ensure that: (i) the Nyquist frequency ($0.5 f_s$) is much higher than the fundamental natural frequencies of the devices [37]; and (ii) a sufficient number (100–200) of points are collected for fitting the resonance peak. The latter can be increased by extending the recording time, but the measurement becomes more susceptible to sporadic extrinsic noise and temperature fluctuations. Hence, several full cycles of measurement and analysis were conducted to determine the appropriate recording time for our devices. Five samples of noise were recorded for each specimen. In addition, for one device (Specimen 3), noise was acquired for various durations from 90 to 130 seconds to quantify the effects of recording time on the estimate for damping. After recording, the voltage time series was imported into MATLAB, filtered to remove any offset and linear drift, rescaled to velocity using a conversion factor of 5 mm/s/V, and numerically integrated to obtain the displacement.

B. Power Spectral Density (PSD) of Displacement and Velocity

The next step is to obtain the power spectral density of the displacement and velocity time series. The PSD of finite time signals can be estimated by segmenting the time series using an appropriate window function, computing the Fourier transform of each segment, and then reassembling the transforms. Such approaches (which include the widely used Welch periodogram technique [37]) are computationally efficient but suffer from spectral leakage and a bias in the estimation of the quality factor [38], [39]. Therefore, we employed a direct method (also called the Daniell method) that eliminates spectral leakage by avoiding segmenting. The underlying statistical concepts and numerical implementation of the Daniell method are discussed in detail in Ref. [38]. Briefly, a single Fourier transform of the entire time series is performed; then, the squared magnitude of the transform is averaged in the frequency domain by grouping adjacent frequency bins until the desired signal-to-noise ratio is reached and/or spectral leakage is eliminated. The number of adjacent frequency bins that are averaged together is called the *averaging factor* (α).

C. Analysis of Noise Spectra

Figure 2 shows a representative example of the PSD of displacement and velocity noise. The response contains a prominent peak at the fundamental natural frequency of the microcantilever. Following the discussion in Section II, this is identified as the resonance peak due to thermomechanical noise. A rough initial estimate of the natural frequency is usually sufficient to locate the resonance peak. If further

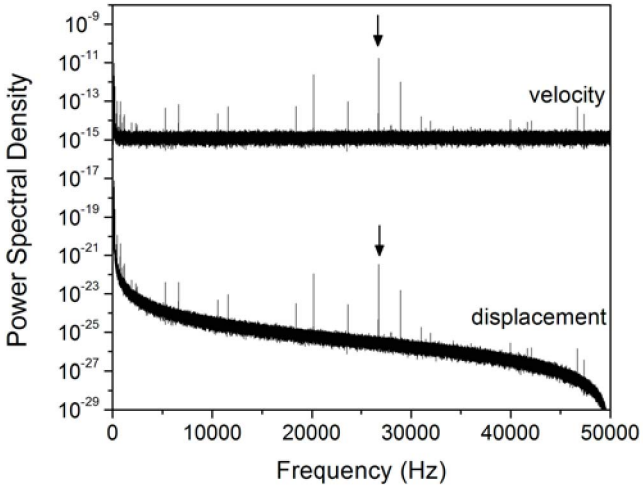

Fig. 2. Power spectral density of velocity noise (in units of $(m/s)^2/Hz$) and displacement noise (in units of m^2/Hz) for a measurement performed on Specimen 1. The arrows point to the fundamental resonance peaks.

verification is required, the measurement can be repeated at atmospheric pressure to check whether the peak broadens due to increased dissipation caused by air damping.

In addition, the noise spectra contain other peaks due to building vibrations, instrumental noise, and aliased higher modes of vibrations. Measurements of the dynamics of the pneumatic air table using a triaxial accelerometer show that the peaks at low frequencies (<100 Hz) are due to building vibrations [36]. To identify the other peaks, we compared the velocity PSD of the four specimens in vacuum (Figure 3(a)) and at atmospheric pressure (Figure 3(b)). As expected, the fundamental resonance peak undergoes a characteristic broadening at atmospheric pressure. The same behavior is exhibited by the aliased higher modes. Thus, a close examination of the noise spectra shows aliased peaks at the following frequencies: 12.8 kHz and 19.8 kHz for Specimen 1; 3.7 kHz and 30.9 kHz for Specimen 2; 25.9 kHz and 41.6 kHz for Specimen 3; 9.9 kHz and 11.5 kHz for Specimen 4. By a process of elimination, we associate all remaining peaks with instrumental noise.

Deconvolution by signal processing is necessary if the thermomechanical resonance overlaps with other noise peaks. This problem was not encountered for any of the four specimens. The resonance peaks are narrow (full width at half maximum ~3 Hz in vacuum) and separated by over 750 Hz from any other peak.

D. Fitting the Resonance Peak

To fit the resonance peak, the PSD of displacement and velocity were expressed as

$$S_x(f) = A_1 + A_2 \frac{\left(\frac{f_0}{Q}\right)}{\left(f_0^2 - f^2\right)^2 + \left(\frac{f^2 f_0^2}{Q^2}\right)};$$
$$S_v(f) = B_1 + B_2 \frac{\left(\frac{f_0}{Q}\right) f^2}{\left(f_0^2 - f^2\right)^2 + \left(\frac{f^2 f_0^2}{Q^2}\right)} \quad (9)$$

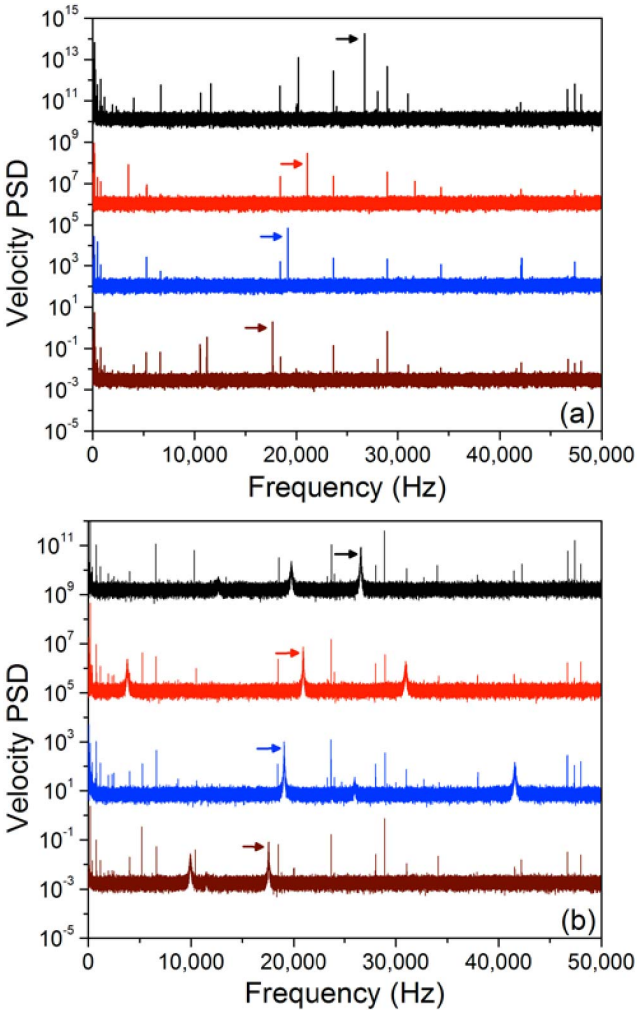

Fig. 3. Velocity power spectral density in (a) vacuum and (b) atmospheric pressure for Specimen 1 (black), Specimen 2 (red), Specimen 3 (blue) and Specimen 4 (brown). The curves are offset for clarity and the arrows point to the fundamental resonance peaks.

The white-noise baseline (A_1, B_1), amplitude (A_2, B_2), fundamental natural frequency (f_0), and quality factor were obtained by implementing a weighted least-squares method using the Levenberg–Marquardt algorithm [37]. The data, fitting curve, and residual errors were plotted to check that the fit captured the baseline, peak shape, and peak height, and that the residuals were uncorrelated [40]–[42]. Figure 4 shows the resonance peak and fitting curves for one representative measurement performed on Specimen 4.

V. Results and Discussion

Table II presents the main results of our study. The natural frequency and quality factor are the averages of five independent measurements, each of 90 seconds in duration. The standard deviation of the natural frequency is less than 1 Hz (that is, one part in 10^5). The entries for Q are shown using the following format: *mean value* (±*relative uncertainty*), where the relative uncertainty is the standard deviation reported as a percentage of the mean.

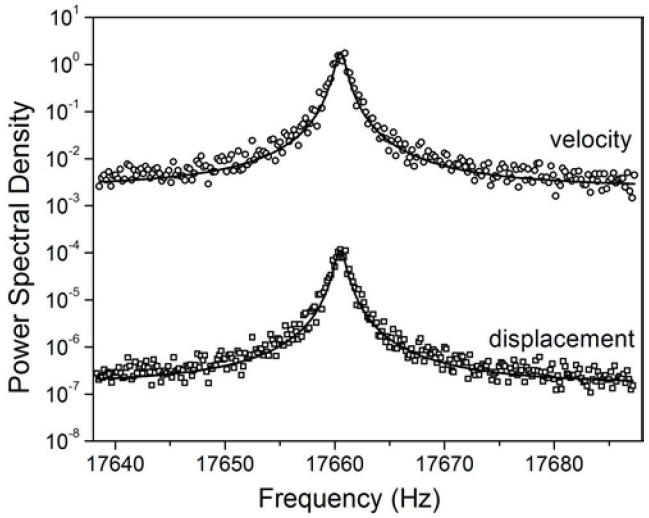

Fig. 4. Resonance peaks in the velocity PSD (in units of $(\mu m/s)^2/Hz$) and displacement PSD (in units of nm^2/Hz) for a measurement performed in vacuum on Specimen 4. The black lines were obtained by fitting Eq.(9) to the resonance peaks.

TABLE II
ESTIMATES FOR NATURAL FREQUENCY (f_0) AND QUALITY FACTOR (Q) OBTAINED BY ANALYZING THE VELOCITY PSD, $S_v(f)$, AND DISPLACEMENT PSD, $S_x(f)$

	Velocity PSD		Displacement PSD	
	f_0 (Hz)	Q	f_0 (Hz)	Q
Specimen 1	26,743	20.3×10^4 (±6%)	26,743	24.5×10^4 (±18%)
Specimen 2	21,045	6.0×10^4 (±18%)	21,045	5.8×10^4 (±19%)
Specimen 3	19,150	10.9×10^4 (±26%)	19,150	9.5×10^4 (±15%)
Specimen 4	17,660	1.8×10^4 (±6%)	17,660	1.8×10^4 (±8%)

The precision of our measurements is influenced by: (i) intrinsic errors associated with estimating the PSD using finite time-series of stochastic fluctuations and (ii) uncertainties associated with fit parameters obtained using least-squares analysis [37]–[40]. Sader *et al.* [40] recommended statistical analysis of multiple independent measurements because the goodness-of-fit of a single measurement may not provide an estimate of uncertainty even when the analysis results in an apparently excellent fit to measurements. Accordingly, we use the relative uncertainty, which ranges from 6% to 26%, as the measure of precision.

As noted earlier, the precision is not affected by uncertainties in beam geometry, material properties, and structural stiffness, or by the details of the mechanisms responsible for dissipation. Instead, we must consider three factors that are integral to the measurement and analysis of thermomechanical resonance peaks. The first is the time for which noise is recorded. We acquired data for 90 s, and this duration was determined based on a trade-off between collecting a sufficiently large number of measurements in the vicinity of the resonance peak while avoiding errors due to sporadic extrinsic noise and drift. As a check, we performed additional measurements in which noise was acquired for various intervals between 90 s and 130 s for one device (Specimen 3). Over this range of recording times, the mean value of Q varied by 8% ($10.4\times10^4 - 11.3\times10^4$) and the standard deviation was typically 20% of the mean.

TABLE III
EFFECTS OF THE AVERAGING FACTOR ON FITTING AND ESTIMATION

α	# of fit points	Frequency resolution	f_0	Q
9	234	0.10 Hz	19,150 Hz	9.50×10^4
11	191	0.12 Hz	19,150 Hz	8.87×10^4
13	163	0.14 Hz	19,150 Hz	9.43×10^4
15	141	0.17 Hz	19,150 Hz	8.95×10^4
17	124	0.19 Hz	19,150 Hz	9.07×10^4

The second is the averaging factor (α) used for computing the PSD using the Daniell method. The variance can be reduced by increasing α, but this is achieved at the expense of degrading the frequency resolution and reducing the number of points available for fitting the resonance peak. Table III quantifies these effects for one representative analysis of the displacement PSD obtained from a measurement performed on Specimen 3. For $\alpha < 9$, the peak was not sufficiently smooth and it was not possible to fit Eq.(9) using the weighted least-squares method. As α increased from 9 to 17, the number of fit points reduced, the frequency resolution was degraded, and Q varied by ~7%. Notably, there was no systematic bias in the estimate for Q over this range, which is the primary motivation for using the Daniell method.

The third factor is the fitting of a sharp resonance peak which makes the estimate sensitively dependent on a small fraction of data points for low-loss devices with $Q > 10^5$. Typically, the PSD contains over 10^6 points but only ~100 are used for fitting the resonance peak. Further, the value of Q is influenced most by ~10 points that lie between the half-power points and the peak. The higher the Q, the sharper the resonance peak, and the smaller the number of points that control the fit parameters. One approach for quantifying these effects is to compare results obtained by fitting the displacement PSD and the velocity PSD. For Specimens 2, 3 and 4, the two estimates are in good agreement which suggests that it is sufficient to fit either the velocity PSD or the displacement PSD for devices with $Q < 10^5$. For Specimen 1, however, it was necessary to use higher averaging factors to fit the velocity PSD compared to the displacement PSD, which lead to differences in frequency resolution and fit parameters. Hence, the displacement PSD was used to estimate Q for this specimen.

Approaches for quantifying the absolute accuracy of damping in high-Q microresonators are not yet available. To our knowledge, no study has yet presented a detailed comparison of damping in well-characterized specimens using two different techniques. As a first step towards filling this gap, we assess the relative accuracy of noise-based estimates

(Table II) by comparison with values of the log decrement obtained using the standard technique of free decay (Table I). A close comparison of the two sets of measurements is possible because the same well-characterized devices, apparatus (precision-machined clamps, vacuum chamber, and vibration isolation systems), and instrumentation (LDV) were used for measuring free decay and noise. Thermomechanical noise overestimates free decay by 27% for Specimen 1 and 7% for Specimen 2, and underestimates by 18% for Specimen 3 and 25% for Specimen 4. Variations in experimental conditions (for example, attaching the specimens to the clamps) can contribute to these differences. Measurements over a larger set of materials, structures, frequencies and quality factors are required to establish whether there are any fundamental limits to the accuracy of noise-based estimates of damping.

VI. Conclusion

In this paper, we focused on a technique for estimating damping in microresonators by measuring thermomechanical noise using laser Doppler vibrometry. Commercial LDVs cannot yet characterize in-plane modes or bulk modes; hence, the technique is currently limited to out-of-plane modes of microresonators. The measurement does not require the use of an actuator, and damping can be estimated without using values for beam dimensions, material properties, or structural stiffness. The various factors involved in recording thermomechanical noise, computing the power spectral density, and fitting the resonance peak were discussed in detail. A notable feature of our approach is the use of a direct method for computing the power spectral density, thereby avoiding any estimation bias resulting from segmenting the data in the time domain. The implementation of the protocol was demonstrated by characterizing damping at room temperature and low pressure in a set of four silicon-based microcantilevers with natural frequencies ranging from 17.6 to 26.7 kHz and quality factors ranging from 2×10^4 to 2×10^5.

Our results can be combined with earlier studies to compare the relative merits and limitations of *free decay*, *harmonic excitation*, and *thermomechanical noise* for measuring damping at the natural frequency. In the free decay technique, damping is estimated by fitting the envelope of decaying oscillations to obtain the logarithmic decrement. The number of fit points scales as the quality factor which makes free decay the technique of choice for precision measurements of damping in low-loss devices with $Q > 10^3$. Free decay is widely used for fundamental studies of damping and internal friction (see, for example, [2], [3], [26], [27]). The main limitations are the need for an actuator to initiate measurement and a loss of precision for highly damped devices [43]. Both limitations can be overcome by using thermomechanical noise to estimate damping over a wide range ($1 < Q < 10^6$). In general, however, noise-based estimates are less precise than free decay due to uncertainties caused by: (i) the estimation of the power spectral density of thermomechanical noise from finite time series of stochastic fluctuations and (ii) fitting a resonance peak to determine the quality factor. For $Q > 10^5$, the fit is sensitive to measurement errors in a small set of data points (usually less than 10) that lie between the resonance peak and the half-power points. For $Q < 10$, the challenge is to identify a shallow and broad peak, and fit it with a function that accounts for the frequency dependence of viscous damping [44].

Harmonic excitation has three major limitations. First, an external actuator is required to apply a harmonic force of constant amplitude over the full spectrum of measurement. Second, the device can be driven into the nonlinear regime due to interactions with the actuator [1] and large displacements at resonance for high-Q devices [45]. Finally, as in the case of thermomechanical noise, errors are incurred when sharp resonance peaks are fit to determine the quality factor of low-loss devices. For all these reasons, harmonic excitation is usually not preferred for precision measurements and fundamental studies of damping and internal friction in high-Q devices.

Acknowledgment

The authors would like to thank G. Sosale, P. Grutter, J. Sader, and A. Parameswaran for valuable suggestions and discussions. The devices were fabricated at the NanoTools Microfabrication Facility at McGill University.

References

[1] S. D. Senturia, *Microsystem Design*. Boston, MA, USA: Kluwer, 2001.
[2] G. Harry, T. P. Bodiya, and R. DeSalvo, *Optical Coatings and Thermal Noise in Precision Measurement*. Cambridge, U.K.: Cambridge Univ. Press, 2012.
[3] A. S. Nowick and B. S. Berry, *Anelastic Relaxation in Crystalline Solids*. New York, NY, USA: Academic, 1972.
[4] E. J. Graesser and C. R. Wong, "The relationship between traditional damping measures for materials with high damping capacity: A review," in *M3D: Mechanics and Mechanisms of Material Damping*, vol. 1169, V. K. Kinra and A. Wolfenden, Eds. Philadelphia, PA, USA: ASTM, 1992, pp. 316–343.
[5] H. B. Callen and T. A. Welton, "Irreversibility and generalized noise," *Phys. Rev.*, vol. 83, no. 1, pp. 34–40, 1951.
[6] H. B. Callen and R. F. Greene, "On a theorem of irreversible thermodynamics," *Phys. Rev.*, vol. 86, no. 5, pp. 702–710, 1952.
[7] P. R. Saulson, "Thermal noise in mechanical experiments," *Phys. Rev. D*, vol. 42, no. 8, pp. 2437–2445, 1990.
[8] Y. Levin, "Internal thermal noise in the LIGO test masses: A direct approach," *Phys. Rev. D*, vol. 57, no. 2, pp. 659–663, 1998.
[9] T. B. Gabrielson, "Mechanical-thermal noise in micromachined acoustic and vibration sensors," *IEEE Trans. Electron. Devices*, vol. 40, no. 5, pp. 903–909, May 1993.
[10] M. Kajima, N. Kusumi, S. Moriwaki, and N. Mio, "Wideband measurement of mechanical thermal noise using a laser interferometer," *Phys. Lett. A*, vol. 264, no. 4, pp. 251–256, 1999.
[11] P. Paolino and L. Bellon, "Frequency dependence of viscous and viscoelastic dissipation in coated microcantilevers from noise measurement," *Nanotechnology*, vol. 20, no. 40, pp. 405705-1–405705-8, 2009.
[12] E. Serra, A. Borrielli, F. S. Cataliotti, F. Marin, F. Marino, A. Pontin, *et al.*, "Ultralow-dissipation micro-oscillator for quantum optomechanics," *Phys. Rev. A*, vol. 86, no. 5, pp. 051801R-1–051801R-5, 2012.
[13] D. Rugar and P. Grutter, "Mechanical parametric amplification and thermomechanical noise squeezing," *Phys. Rev. Lett.*, vol. 67, no. 6, pp. 699–702, 1991.
[14] O. Pfeiffer, C. Loppacher, C. Wattinger, M. Bammerlin, U. Gysin, M. Guggisberg, *et al.*, "Using higher flexural modes in non-contact force microscopy," *Appl. Surf. Sci.*, vol. 157, no. 4, pp. 337–342, 2000.
[15] M. V. Salapaka, H. S. Bergh, J. Lai, A. Majumdar, and E. McFarland, "Multi-mode noise analysis of cantilevers for scanning probe microscopy," *J. Appl. Phys.*, vol. 81, no. 6, pp. 2480–2487, 1997.
[16] A. K. Kar and M. A. George, "Improved detection of thermally induced higher resonance modes and harmonics of a microcantilever," *J. Appl. Phys.*, vol. 94, no. 7, pp. 4626–4631, 2003.
[17] G. A. Matei, E. J. Thoreson, J. R. Pratt, D. B. Newell, and N. A. Burnham, "Precision and accuracy of thermal calibration of atomic force microscopy cantilevers," *Rev. Sci. Instrum.*, vol. 77, no. 8, pp. 083703-1–083703-6, 2006.

[18] J. L. Hutter and J. Bechhoefer, "Calibration of atomic-force microscope tips," *Rev. Sci. Instrum.*, vol. 64, pp. 1868–1873, Apr. 1993.
[19] A. Mehta, S. Cherian, D. Hedden, and T. Thundat, "Manipulation and controlled amplification of Brownian motion of microcantilever sensors," *Appl. Phys. Lett.*, vol. 78, no. 11, pp. 1637–1639, 2001.
[20] A. Gupta, D. Akin, and R. Bashir, "Single virus particle mass detection using microresonators with nanoscale thickness," *Appl. Phys. Lett.*, vol. 84, no. 11, pp. 1976–1978, 2004.
[21] B. Ohler, "Cantilever spring constant calibration using laser Doppler vibrometry," *Rev. Sci. Instrum.*, vol. 78, no. 6, pp. 063701-1–063701-5, 2007.
[22] R. S. Gates and J. R. Pratt, "Accurate and precise calibration of AFM cantilever spring constants using laser Doppler vibrometry," *Nanotechnology*, vol. 23, no. 37, pp. 375702–375713, 2012.
[23] J. E. Sader, J. A. Sanelli, B. D. Adamson, J. P. Monty, X. Wei, S. A. Crawford, *et al.*, "Spring constant calibration of atomic force microscope cantilevers of arbitrary shape," *Rev. Sci. Instrum.*, vol. 83, no. 10, pp. 103705-1–103705-16, 2012.
[24] J. R. Lozano, D. Kiracofe, J. Melcher, R. Garcia, and A. Raman, "Calibration of higher eigenmode spring constants of atomic force microscope cantilevers," *Nanotechnology*, vol. 21, no. 46, pp. 465502-1–465502-7, 2010.
[25] C. Rembe, G. Siegmund, H. Steger, and M. Wortge, "Measuring MEMS in motion by laser Doppler vibrometry," in *Optical Inspection of Microsystems*, W. Osten, Ed. Boca Raton, FL, USA: CRC Press, 2007.
[26] R. Lakes, *Viscoelastic Materials*. Cambridge, U.K.: Cambridge Univ. Press, 2009.
[27] G. Sosale, D. Almecija, K. Das, and S. Vengallatore, "Mechanical spectroscopy of nanocrystalline aluminum films: Effects of frequency and grain size on internal friction," *Nanotechnology*, vol. 23, no. 15, pp. 155701-1–155701-7, 2012.
[28] R. Lifshitz and M. L. Roukes, "Thermoelastic damping in micro- and nanomechanical systems," *Phys. Rev. B*, vol. 61, no. 8, pp. 5600–5609, 2000.
[29] S. Prabhakar and S. Vengallatore, "Theory of thermoelastic damping in micromechanical resonators with two-dimensional heat conduction," *J. Microelectromech. Syst.*, vol. 17, no. 2, pp. 494–502, 2008.
[30] K. Kunal and N. R. Aluru, "Akhiezer damping in nanostructures," *Phys. Rev. B*, vol. 84, no. 24, pp. 245450-1–245450-8, 2011.
[31] S. Vengallatore, "Gorsky damping in nanomechanical structures," *Scripta Mater.*, vol. 52, no. 12, pp. 1265–1268, 2005.
[32] G. Sosale, S. Prabhakar, L. Fréchette, and S. Vengallatore, "A microcantilever platform for measuring internal friction in thin films using thermoelastic damping for calibration," *J. Microelectromech. Syst.*, vol. 20, no. 3, pp. 764–773, 2011.
[33] K. Das. G. Sosale, and S. Vengallatore, "Design, implementation, and application of a microresonator platform for measuring energy dissipation by internal friction in nanowires," *Nanotechnology*, vol. 23, no. 50, pp. 505703–505709, 2012.
[34] G. Sosale, K. Das, L. Fréchette, and S. Vengallatore, "Controlling damping and quality factors of silicon microcantilevers by selective metallization," *J. Micromech. Microeng.*, vol. 21, no. 10, pp. 105010–105016, 2011.
[35] S. Joshi, S. Hung, G. Sosale, and S. Vengallatore, "Damping in micromechanical and nanomechanical resonators," in *Proc. 10th Int. Workshop NMC*, Stanford, CA, USA, May 2013, pp. 11–14.
[36] G. Sosale, "A microcantilever platform for measuring internal friction in thin films using thermoelastic damping for calibration," Ph.D. dissertation, Dept. Mech. Eng., McGill University, Montreal, QC, Canada, 2011.
[37] W. H. Press, S. A. Teukolsky, W. T. Vetterling, and B. P. Flannery, *Numerical Recipes: The Art of Scientific Computing*, Cambridge, U.K.: Cambridge Univ. Press, 2007.
[38] A. Labuda, M. Lysy, W. Paul, Y. Miyahara, P. Grutter, R. Bennewitz, *et al.*, "Stochastic noise in atomic force microscopy," *Phys. Rev. E*, vol. 86, no. 3, pp. 031104-1–031104-18, 2012.
[39] J. E. Sader, J. Sanelli, B. D. Hughes, J. P. Monty, and E. J. Bieske, "Distortion in the thermal noise spectrum and quality factor of nanomechanical devices due to finite frequency resolution with applications to the atomic force microscope," *Rev. Sci. Instrum.*, vol. 82, no. 9, pp. 095104-1–095104-10, 2011.
[40] J. E. Sader, B. D. Hughes, J. A. Sanelli, and E. J. Bieske, "Effect of multiplicative noise on least-squares parameter estimation with applications to the atomic force microscope," *Rev. Sci. Instrum.*, vol. 83, no. 5, pp. 055106-1–055106-6, May 2012.
[41] S. F. Norrelykke and H. Flyvbjerg, "Power spectrum analysis with least-squares fitting: Amplitude bias and its elimination, with application to optical tweezers and atomic force microscope cantilevers," *Rev. Sci. Instrum.*, vol. 81, no. 7, pp. 075103-1–075103-16, 2010.
[42] P. R. Bevington and D. K. Robinson, *Data Reduction and Error Analysis for the Physical Sciences*, 2nd ed. New York, NY, USA: McGraw-Hill, 1992.
[43] A. Rivière, "Measurement of high damping: Technique and analysis," *J. Alloys Compounds*, vol. 355, nos. 1–2, pp. 201–206, 2003.
[44] J. W. M. Chon, P. Mulvaney, and J. E. Sader, "Experimental validation of theoretical models for the frequency response of atomic force microscope cantilever beams immersed in fluids," *J. Appl. Phys.*, vol. 87, no. 8, pp. 3978–3988, 2000.
[45] H. W. C. Postma, I. Kozinsky, A. Husain, and M. L. Roukes, "Dynamic range of nanotube- and nanowire-based electromechanical systems," *Appl. Phys. Lett.*, vol. 86, no. 22, pp. 223105-1–223105-3, 2005.

Ottoleo Kuter-Arnebeck received the B.Sc. degree in mechanical engineering from Carnegie Mellon University, Pittsburgh, PA, in 2009. He is currently working towards the Ph.D. degree in the Department of Mechanical Engineering at McGill University, Montreal, QC, Canada. His research focuses on the dynamics and applications of microscale and nanoscale resonators. He is also interested in the application of engineering and micro- and nanofabrication to the fine arts.

Mr. Kuter-Arnebeck is the recipient of a Vanier Canada Graduate Scholarship from the Natural Sciences and Engineering Research Council of Canada.

Aleksander Labuda received the Ph.D. degree in physics from McGill University, Montreal, QC, Canada in 2012 with a thesis in the field of condensed matter physics. His expertise lies in atomic force microscopy (AFM), with interests in AFM design for extending current technological capabilities and improving imaging performance; AFM methodology for developing new measurement techniques; and AFM theory for more accurately relating raw experimental data to true physical quantities.

He is currently working at Asylum Research – an Oxford Instruments Company, developing methods for photothermal excitation of AFM cantilevers, and working on theoretical frameworks for more accurately interpreting AFM signals and achieving the fundamental physical limits of noise.

Surabhi Joshi received the B.Eng. and M.Eng. degrees in mechanical engineering from McGill University, Montreal, QC, Canada, in 2011 and 2013, respectively. She is currently working as a Research Associate at the same institution. Her research focuses on approaches for studying energy dissipation and damping in micro- and nanomechanical systems.

Ms. Joshi was a recipient of the Provost's Graduate Fellowship from McGill University.

Kaushik Das received the B.Eng. degree in metallurgical engineering from Bengal Engineering and Science University, Shibpur, India, in 2005, the M.Eng. degree in materials engineering from Indian Institute of Science, Bangalore, India, in 2007, and the Ph.D. degree in mechanical engineering from McGill University, Montreal, QC, Canada, in 2012.

He is currently working as a process development engineer at the MiQro Innovation Collaborative Centre (C2MI), Bromont, QC, Canada. His research is focused on experimental approaches to characterize quasi-static and dynamic mechanical properties of advanced nanomaterials in the form of glass-ceramics, polymer nanocomposite films, metallic thin films, and nanowires. Integration of nanomaterials to microsystems is an integral part of his research activities.

Srikar Vengallatore received the B.Tech. degree (with honours) in metallurgical engineering from the Institute of Technology, Banaras Hindu University, Varanasi, India, in 1994, and the Ph.D. degree in materials science from the Massachusetts Institute of Technology (MIT), Cambridge, in 1999.

He worked as a Postdoctoral Associate at MIT from 1999 to 2003, and then joined McGill University, Montreal, QC, Canada, where he is currently a Canada Research Chair and Associate Professor in the Department of Mechanical Engineering. His research focuses on understanding the mechanical properties of materials at micrometer and nanometer length scales, and then translating this knowledge to practice by designing and developing microsystems (MEMS) for sensing, signal processing, scanning probe microscopy, energy harvesting and portable power generation.

Dr. Vengallatore is a member of Alpha Sigma Mu and Sigma Xi. He was the recipient of the Class of '44 Award for Outstanding Teaching in 2007 and the Early Career Research Excellence Award in 2009.